CHEMPHYSCHEM

Noncovalent Complexes between Dimethyl Ether and Formic Acid—An Ab Initio and Matrix Isolation Study

Elsa Sánchez-García,[a] Marc Studentkowski,[a] Luis A. Montero,[b] and Wolfram Sander*[a]

The complexes formed by noncovalent interactions between formic acid and dimethyl ether are investigated by ab initio methods and characterized by matrix isolation spectroscopy. Six complexes with binding energies between −2.26 and −7.97 kcal mol^{-1} (MP2/cc-pVTZ + zero point vibrational energy + basis set superposition erros) are identified. The two strongest bound complexes are, within a range of 0.3 kcal mol^{-1}, isoenergetic. The binding in these six dimers can be described in terms of OH···O, C=O···H, C–O···H and CH···O interactions. Matrix isolation spectroscopy allowed to characterize the two strongest bound complexes by their infrared spectra.

Introduction

Hydrogen-bonded complexes have been subject to a large number of studies in chemistry and life sciences. Oxygen atoms as hydrogen bond acceptors are of particular interest since they play a key role in biological processes. Formic acid (FA) is one of the simplest organic molecules forming hydrogen bonds in the gaseous, liquid and solid state, and it is therefore used as a model to study hydrogen bond interactions in biological systems. The proton transfer mechanism of the FA dimer has been extensively described,[1–6] and studies of the complexes of FA with acetylene and FA with water were carried out in our group using matrix isolation spectroscopy and ab initio methods.[7,8] Complexes involving the interactions of ethers with molecules of biological interest are also described in literature,[9–13] including matrix isolation and ab initio studies of dimethyl ether (DME) complexes with water,[14] methanol,[15,16] hydrogen peroxide[17] and hydracids.[18] Herein, we discuss the calculated structures, binding energies and vibrational properties of DME–FA complexes using both matrix isolation techniques and ab initio calculations. The DME–FA system exhibits classical as well as weak OH···O, C=O···H, C–O···H and CH···O hydrogen-bonding interactions, making these complexes interesting for theoretical and experimental research.

Experimental and Computational Section

Matrix isolation experiments were performed by standard techniques using an APD CSW-202 Displex closed cycle helium refrigerator. Formic Acid (Acros Organics) was distilled two times, dried over molecular sieve (4 Å) and degassed several times by the freeze-pump-thaw method before mixing with argon. Formic acid (FA) and dimethyl ether (DME) were premixed with argon in a glass mixing chamber using standard manometric methods. About 0.5–4 mbar of FA were mixed with 0.5–5 mbar of DME and diluted with 600–850 mbar of argon in a two-liter glass bulb. Deposition was done on a CsI substrate at 13 K. The matrix was annealed at 25, 30 and 35 K by keeping at that temperature for up to 60 minutes and cooled back to 13 K before recording spectra. Spectra were recorded on a Bruker IFS 66 FTIR spectrometer at 0.5 cm^{-1} resolution in the range of 400–4000 cm^{-1}.

Computational Methods: The ab initio computations were performed using the Gaussian 98[19] and Gaussian 03[20] series of programs. The equilibrium geometries and vibrational frequencies were calculated at the SCF level including second-order Møller–Plesset perturbation theory, MP2.[21] Pople's 6-31G(d,p) basis set, the extended valence triple ζ basis set augmented with diffuse and polarization functions 6-311++G(d,p), and Dunning's correlation consistent triple ζ basis set cc-pVTZ[22–24] were used.

The stabilization energies were calculated by subtracting the energies of the monomers from those of the complexes and including zero point vibrational ernergy (ZPE) corrections to discard other than electronic terms in the energy comparisons. The energies were also corrected for the basis set superposition errors (BSSE) using the counterpoise (CP) scheme of Boys and Bernardi.[25]

The multiple minima hypersurface (MMH) approach[8,26–28] provides a very reliable procedure for searching minima in weakly interacting complexes and was used to localize the minima in the FA–DME system. One thousand randomly arranged FA–DME clusters were generated as starting points, and the resulting geometries were optimized and analyzed using PM3 and AM1[29–31] approximate quantum-mechanical Hamiltonians. It is important to point out that these semiempirical results provide a preliminary overview of the FA–DME interactions only. After geometrical analysis both PM3 and AM1 lead to the same minima which were further refined using ab initio methods.

[a] *E. Sánchez-García, M. Studentkowski, Prof. Dr. W. Sander*
Lehrstuhl für Organische Chemie II, Ruhr-Universität Bochum
44780 Bochum (Germany)
Fax: (+49) 234-3214353
E-mail: wolfram.sander@rub.de

[b] *Prof. Dr. L. A. Montero*
Laboratorio de Química Computacional y Teórica
Facultad de Química, Universidad de la Habana, 10400 (Cuba)

  DOI: 10.1002/cphc.200400430

Results and Discussion

Geometries and Binding Energies

Six DME–FA complexes **A**–**F** were found at the MP2 level of theory with the 6-311++G(d,p) and cc-pVTZ basis sets (Figure 1). For all complexes the geometries are almost independent of the basis sets used, therefore we discuss hydrogen bond distances and angles calculated at the MP2/cc-pVTZ level of theory only. The calculated binding energies (Table 1) predict complexes **A** and **B** as the lowest minima, being both very close in energy. During the optimization process the second enantiomer of complex **B** was also found. According to the calculated binding energies complexes **C**–**F** are much less stable.

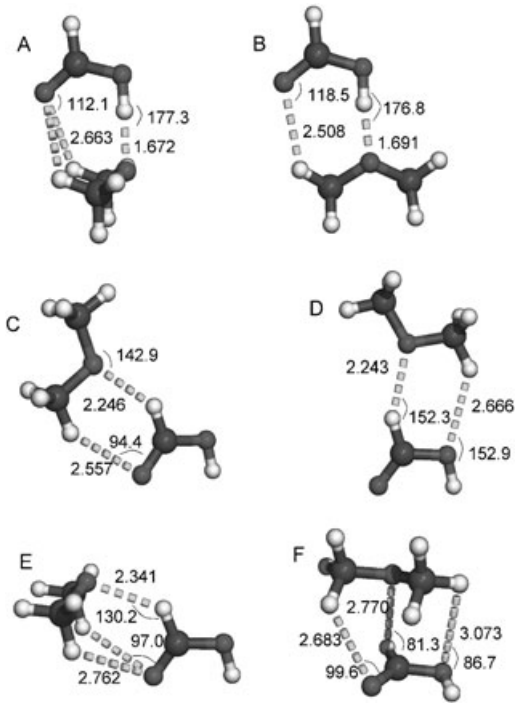

Figure 1. *The calculated structures with hydrogen bond lengths (Å) and some hydrogen bond angles (degree) of the FA–DME complexes **A**–**F** at the MP2/cc-pVTZ level of theory.*

Four basic types of interactions (1)–(4) can be differentiated in the FA–DME complexes:

1) $HC(=O)OH\cdots O(CH_3)_2$ interaction between the hydroxyl hydrogen atom of FA and the ether oxygen atom of DME.
2) $HOC(H)=O\cdots HCH_2OCH_3$ interaction between the carbonyl oxygen atom of FA and the hydrogen atoms of DME.
3) $HOC(=O)H\cdots O(CH_3)_2$ interaction between the aldehyde hydrogen atom of FA and the ether oxygen atom of DME.
4) $O=C(H)O(H)\cdots HCH_2OCH_3$ interaction between the hydroxyl oxygen atom of FA and the hydrogen atoms of DME.

Complexes **A** and **B** show the same type of interactions (1) and (2). The hydrogen atom of the OH group of the FA interacts with the ether oxygen atom of DME at hydrogen bond distances of 1.672 Å and 1.691 Å for the dimers **A** and **B**, respectively. The difference between these complexes is caused by the interaction (2). In dimer **A** the C=O group of FA interacts simultaneously with two hydrogen atoms of DME at distances of 2.663 Å, while in dimer **B** the C=O group of FA is approaching only one hydrogen atom of the DME with a distance of 2.508 Å.

With the 6-311++G(d,p) and cc-pVTZ basis sets (without including ZPE and BSSE corrections) the differences between the binding energies of complexes **A** and **B** ($\Delta E_B - \Delta E_A$, $\Delta\Delta E_{BA}$) are 0.54 and 0.92 kcal mol^{-1}, respectively. After including BSSE and ZPE corrections these differences are reduced to −0.29 kcal mol^{-1} (6-311++G(d,p)) and 0.16 kcal mol^{-1} (cc-pVTZ) (Table 1). With the 6-311++G(d,p) basis set including all corrections the binding energies for dimers **A** and **B** are −6.40 and −6.69 kcal mol^{-1}, respectively. This is due to the large BSSE error for complex **A** with the 6-311++G(d,p) basis set which considerably lowers the binding energy of complex **A** compared to **B**.

Comparing the structures of the DME–FA complexes **A** and **B** with the DME–methanol complex reported in literature[15,16] reveals large similarities. Han and Kim[16] calculated at the MP2/6-31+G** level of theory the hydrogen bond distance $CH_3OH\cdots O(CH_3)_2$ of 1.855 Å and the OH···O hydrogen bond angle of 177.2°, in good agreement with our OH···O hydrogen bond distances of 1.672 Å and 1.691 Å, respectively, and OH···O bond angles of 177.3° and 176.8°, respectively, for complexes **A** and **B** (MP2/cc-pVTZ).

A cyclic dimer of FA–water has been described experimentally by Astrand et al.[32] and Priem et al.[33] It is also interesting to compare our complexes with the geometries of the recently calculated FA–water complexes by Zhou et al.[34] The most stable FA–water complex found by these authors is a cyclic complex with both FA and water acting as hydrogen donor

Table 1. *Calculated binding energies including ZPE and BSSE corrections [in kcal mol^{-1}] of the FA–DME complexes **A**–**F**.*

Complex	MP2/6-311G++(d,p)					MP2/cc-pVTZ				
	ΔE	ZPE	BSSE	$\Delta E_{(ZPE)}$	$\Delta E_{(ZPE+BSSE)}$	ΔE	ZPE	BSSE	$\Delta E_{(ZPE)}$	$\Delta E_{(ZPE+BSSE)}$
A	−11.41	1.63	3.38	−9.78	−6.40	−12.23	1.50	2.76	−10.73	−7.97
B	−10.87	1.43	2.75	−9.44	−6.69	−11.31	1.28	2.22	−10.03	−7.81
C	−4.19	0.64	1.13	−3.55	−2.42	−5.03	0.73	1.43	−4.30	−2.87
D	−3.90	0.53	1.08	−3.37	−2.29	−4.47	0.59	1.22	−3.38	−2.66
E	−4.30	0.77	1.62	−3.53	−1.91	−5.26	0.82	1.78	−4.44	−2.66
F	−4.35	0.93	2.26	−3.42	−1.16	−5.01	0.91	1.84	−4.10	−2.26

and acceptor. The HC(O)OH···OH_2 and HOC(H)=O···HOH distances were calculated to 1.792 Å and 2.144 Å, respectively, at the MP2/6-311++G(d,p) level of theory. It is remarkable how this cyclic FA–water complex shows the same type (1) and (2) interactions as the DME–FA complexes **A** and **B**.

Zhou et al. reported two additional more weakly bound FA–water dimers. One of those is a HOC(H)=O···HOH complex with a calculated C=O···H bond angle of 99.8° and an O···H distance of 2.053 Å. Its geometry is very similar to the DME–FA dimer **C**, where the calculated C=O···H distance is 2.666 Å and the COH hydrogen bond angle is 95.5° (for comparison with ref. [34] calculated at the MP2/6-311++G(d,p) level of theory). The DME–FA complex **C** is stabilized by both interactions (2) and (3) and the C–H···O distance of 2.257 Å is calculated.

The other FA–water complex found by Zhou et al. is the OC(H)O(H)···HOH complex, where the O···H_{water} distance is 2.204 Å and the (H)O···H_{water} angle is 147.6°. DME–FA dimer **D** exhibits a similar geometry, the calculated O=C(H)O(H)···H-CH_2OCH_3 distance is 2.812 Å and the (H)O···H hydrogen bond angle is 154.5° [MP2/6-311++G(d,p)]. Complex **D** shows interactions (3) and (4), the O=C(OH)H···O$(CH_3)_2$ distance is 2.230 Å. Comparing the MP2/cc-pVTZ geometries of complexes **C** and **D** (Figure 1) with their MP2/6-311++G(d,p) geometries (as discussed above) reveals that the structures of these complexes are almost independent of the basis set used in the calculations.

Dimer **E** is stabilized by interactions (2) and (3) and dimer **F** by interactions (2), (3) and (4). The calculated MP2/cc-pVTZ+ZPE+BSSE binding energies of complexes **C**–**F** are similar and around 5 kcal mol^{-1} smaller than the binding energies of complexes **A** and **B**. This can be rationalized by the lack of the strongest interaction (1) in complexes **C**–**F**.

Geometry Optimization Including BSSE

To investigate the influence of the basis set superposition errors (BSSE) on the geometries of the complexes, the geometries of complexes **A**–**E** were optimized at the MP2/6-31G(d,p) level of theory using the counterpoise (CP) scheme of Boys and Bernardi[25] during the optimization process. In addition, the geometries were optimized without BSSE at the same level of theory in order to evaluate the influence of BSSE on the calculated energies as well as the geometries. The small 6-31G-(d,p) basis set was selected since the BSSE is here more pronounced compared to larger basis sets and in addition the calculations are less demanding. Complexes **A**–**D** are discussed here to illustrate different types of dimers including strong and weak interactions and similar and different binding energies (Tables 2 and 3).

The C=O and O–H bond distances in the FA part of the complexes and the C–O distances in the DME part are almost not effected by the inclusion of BSSE during the optimization. In all cases the difference in these bond distances was in the order of 10^{-3} Å (Table 2). The OH···O, C=O···H, CH···O and C–O···H intermolecular distances [interactions (1), (2), (3) and (4), respectively] are more influenced by BSSE. The weak interactions (2) and (4), where DME hydrogen atoms are involved, exhibit the largest changes. Thus, the C=O···H and C–O···H distances increase by about 0.2–0.3 Å when BSSE is considered during the optimization. Despite these variations the basic geometries and interactions in the FA–DME complexes do not change. The calculated binding energies of **A**–**D** (Table 3) are also almost independent of using BSSE corrections during geometry optimization, which clearly demonstrates that consideration of BSSE during geometry optimization is not mandatory (Table 3). The large BSSE in complex **A** lowers its binding energies below that of complex **B**. However, both complexes are still very close in energy and more stabilized than the other dimers. These results are similar to that obtained with the MP2/6-311++G(d,p) level of theory described above.

Intramolecular Distances and Vibrational Frequencies

Compared to the monomers, intramolecular distances and vibrational frequencies in the complexes are distorted as a consequence of the intermolecular interactions. For the monomers

Table 2. *Comparison of selected intramolecular and intermolecular distances in the FA–DME complexes **A**–**D** at the MP2/6-31G(d,p) level of theory. The results from geometry optimizations without and including BSSE corrections are compared.*

	MP2/6-31G (d,p)							
	Optimization with BSSE				Optimization without BSSE			
	A	**B**	**C**	**D**	**A**	**B**	**C**	**D**
Intramolecular distances								
r(C=O)$_{FA}$	1.219	1.218	1.216	1.215	1.222	1.220	1.218	1.214
r(O–H)$_{FA}$	0.989	0.986	0.972	0.972	0.995	0.991	0.972	0.972
r(C–O)$_{DME}$	1.425	1.423	1.419	1.417	1.429	1.427	1.421	1.419
r(C–O)[e]	–	1.419	1.415	1.416	–	1.421	1.416	1.416
Intermolecular distances								
OH···O[a]	1.801	1.804	–	–	1.706	1.725	–	–
C=O···H[b]	2.922	2.589	2.751	–	2.596	2.457	2.526	–
CH···O[c]	–	–	2.330	2.315	–	–	2.260	2.252
C–O···H[d]	–	–	–	2.880	–	–	–	2.638

[a] Interaction (1). [b] Interaction (2). [c] Interaction (3). [d] Interaction (4) between FA and DME. [e] C–O bond distance between the DME oxygen atom and the noninteracting methyl group.

Table 3. *Calculated binding energies including BSSE corrections [in kcal mol^{-1}] of the FA–DME complexes **A**–**D** at the MP2/6-31G(d,p) level of theory. The results from geometry optimizations without and including BSSE corrections are compared.*

Complex	MP2/6-31G(d,p)					
	Optimization with BSSE			Optimization without BSSE		
	ΔE	BSSE	ΔE+BSSE	ΔE	BSSE	ΔE+BSSE
A	−12.23	4.05	−8.18	−12.82	5.10	−7.72
B	−11.60	3.26	−8.34	−11.92	3.86	−8.06
C	−4.81	2.07	−2.74	−4.98	2.39	−2.59
D	−4.21	1.72	−2.49	−4.35	1.99	−2.36

the available experimental geometrical data are well reproduced at the MP2/cc-pVTZ and MP2/6-311++G(d,p) levels of theory (Table 4).

The most perturbed vibrational modes in complexes **A** and **B** are the O–H stretching vibrations of the FA molecule (Tables 5 and 6). At the MP2/cc-pVTZ level of theory the frequency shifts in the complexes **A** and **B** are −538 and −449 cm^{-1}, respectively. This reflects the strong interactions between the OH hydrogen atom and the ether oxygen atom in complexes **A** and **B** (Figure 1) which results in an elongation of the OH bonds of approximately 0.025 Å (MP2/cc-pVTZ, Table 4).

The carbonyl stretching frequencies of the FA molecules in complexes **A** and **B** are predicted to be red-shifted by 31 and 24 cm^{-1}, respectively, again reflecting the strong CO···H interaction [contribution (2)]. The C=O bond lengths in dimers **A** and **B** compared to the monomer increase by nearly 0.010 Å. In complex **A**, where the carbonyl oxygen atom of FA interacts with two H atoms of DME, the predicted red-shift of the carbonyl stretching frequency is 7 cm^{-1} larger than in dimer **B** with only one contact.

The C–OH stretching modes of the FA molecules in complexes **A** and **B** are blue-shifted by 89 cm^{-1} and 91 cm^{-1}, respectively, and consequently the C–OH bond lengths are 0.017 Å shorter than in the monomer. The symmetrical and antisymmetrical O–C–O and CH_3 stretching modes of the DME moieties are also perturbed in complexes **A** and **B** as listed in Tables 5 and 6.

Table 4. *Comparison of the selected intramolecular distances of FA, DME, and the FA–DME complexes **A** and **B**.*

	Experiment	MP2/cc-pVTZ			MP2/6-311++G(d,p)		
	Monomer	Monomer	**A**	**B**	Monomer	**A**	**B**
Formic acid							
r(C=O)	1.202(10)[39]	1.203	1.212	1.210	1.205	1.214	1.212
r(O–H)	0.972 (5)[39]	0.969	0.996	0.992	0.969	0.993	0.989
r(C–O)	1.343 (10)[39]	1.346	1.329	1.329	1.348	1.332	1.333
Dimethyl ether							
r(C–O)	1.410[14]	1.408	1.423	1.416[a]	1.411	1.424	1.419[a]
				1.421			1.424
r(C–H) in plane	1.091[14]	1.086	1.086	1.084	1.090	1.090	1.089
r(C–H)	1.100[14]	1.095	1.091	1.092	1.099	1.096	1.096

[a] C–O bond between the DME oxygen atom and the noninteracting methyl group.

Table 5. *The experimental (Ar matrix at 35 K–45 K) and the calculated MP2/cc-pVTZ unscaled vibrational frequencies [in cm^{-1}] of the FA–DME complex **A**, along with the frequency shift in the complex, $\Delta\nu$, from the monomer (in parentheses).*

Experiment			MP2/cc-pVTZ			Assignment
Monomer	Complex **A**		Monomer	Complex **A**		
Formic Acid			Formic Acid			
3550.5	3000.3	(−550.2)	3763.4	3225.1	(−538.3)	ν_{36}:ν(O–H)
1767.3	1735.0	(−32.3)	1818.1	1786.7	(−31.4)	ν_{28}:ν(C=O)
1103.7	1181.9	(78.2)	1136.7	1225.6	(88.9)	ν_{18}:ν(C–O)
635.4	961.6	(326.2)	686.2	1029.7	(343.5)	ν_{11}:γ(O–H) oop[a]
629.2	679.8	(50.6)	629.2	688.4	(59.2)	ν_{10}:δ(O-C=O)
Dimethyl ether			Dimethyl ether			
1098.3	1077.3	(−21.0)	1138.0	1124.4	(−13.6)	ν_{14}:ν_{as}(O–C–O)
925.9	899.9	(−26.0)	970.6	943.4	(−27.2)	ν_{12}:ν_{s}(O–C–O)

[a] oop = out of plane.

*Table 6. The experimental (Ar matrix at 25 K–35 K) and the calculated MP2/cc-pVTZ unscaled vibrational frequencies [in cm^{-1}] of the FA–DME complex **B**, along with the frequency shift in the complex, $\Delta\nu$, from the monomer (in parentheses).*

Experiment			MP2/cc-pVTZ			Assignment
Monomer	Complex **B**		Monomer	Complex **B**		
Formic Acid			Formic Acid			
3550.5	3077.8	(−472.7)	3763.4	3314.6	(−448.8)	ν_{36}:ν(O–H)
1767.3	1741.2	(−26.1)	1818.1	1793.7	(−24.4)	ν_{28}:ν(C=O)
1103.7	1179.4	(75.7)	1136.7	1228.1	(91.4)	ν_{18}:ν(C–O)
635.4	852.8	(217.4)	686.2	933.6	(247.4)	ν_{11}:γ(O–H) oop[a]
629.2	681.5	(52.3)	629.2	693.1	(63.9)	ν_{10}:δ(O–C=O)
Dimethyl ether			Dimethyl ether			
1098.3	1092.0	(−6.3)	1138	1133.1	(−4.9)	ν_{14}:ν_{as}(O–C–O)
925.9	915.2	(−10.7)	970.6	953.2	(−17.4)	ν_{12}:ν_{s}(O–C–O)

[a] oop = out of plane.

Matrix Isolation Studies

Matrix isolation experiments were performed in order to identify aggregates between FA and DME. The experiments were performed by matrix isolation of mixtures of FA and DME in argon at 10 K. Under these conditions (high dilution in argon and slow deposition) mainly the monomers of FA and DME were matrix-isolated. Subsequent annealing of the matrix at temperatures up to 35 K resulted in the formation of complex mixtures of aggregates. The main constitutes of these mixtures were identified as the FA dimer, which has been extensively described in literature,[35–37] and complexes between DME and FA. Small amounts of the dimer of DME were also formed. This dimer was independently obtained by annealing of matrices containing the DME monomer.

The annealing experiments show two new sets of IR bands which are only produced in the presence of both DME and FA, which are thus assigned to mixed FA/DME aggregates. One set is formed on depositing a matrix of FA, DME, and argon in a 1:1:600 ratio. On annealing at 25 K the intensities of these bands slightly increase (Figures 2–6 and Table 6). By comparison with the calculated spectra this aggregate is assigned to dimer **B**. The other set of IR bands requires annealing at 35 K and is assigned to dimer **A** (Table 5). Simultaneously with the increase of bands assigned to dimer **A** the bands assigned to

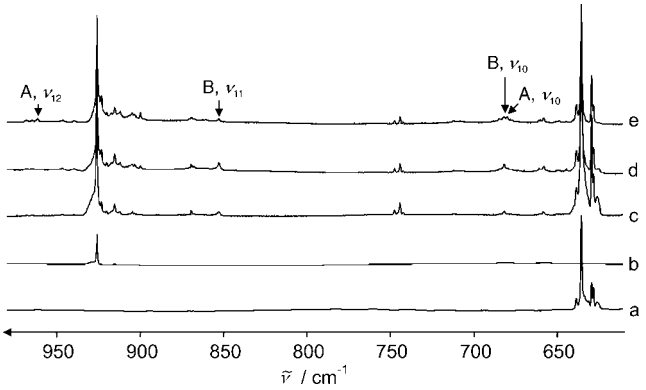

*Figure 2. IR spectra in the range 600–1000 cm^{-1} of FA, DME, and FA/DME mixtures, matrix-isolated in argon. a) FA:Ar ratio 1:600, 13 K. b) DME:Ar ratio 1:600, 13 K. c) FA:DME:Ar ratio 1:1:600, 13 K. d) FA:DME:Ar ratio 1:1:600 after annealing at 25 K. e) FA:DME:Ar ratio 1:2:600 after annealing at 35 K. Vibrational modes assigned to FA/DME complexes are labeled **A** and **B**, respectively (see Tables 5 and 6).*

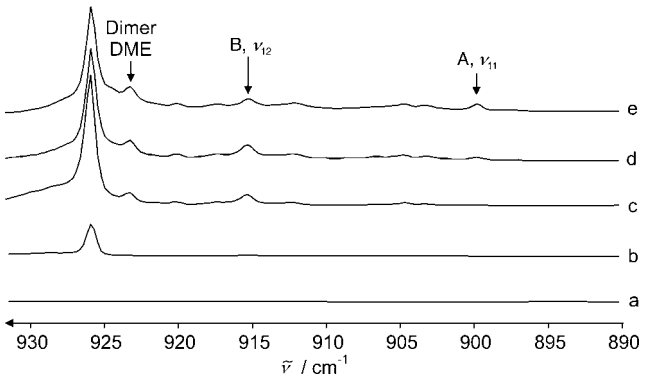

*Figure 3. IR spectra in the range 890–935 cm^{-1} of FA, DME, and FA/DME mixtures, matrix-isolated in argon. a) FA:Ar ratio 1:600, 13 K. b) DME:Ar ratio 1:600, 13 K. c) FA:DME:Ar ratio 1:1:600, 13 K. d) FA:DME:Ar ratio 1:1:600 after annealing at 25 K. e) FA:DME:Ar ratio 1:2:600 after annealing at 35 K. Vibrational modes assigned to FA/DME complexes are labeled **A** and **B**, respectively (see Tables 5 and 6).*

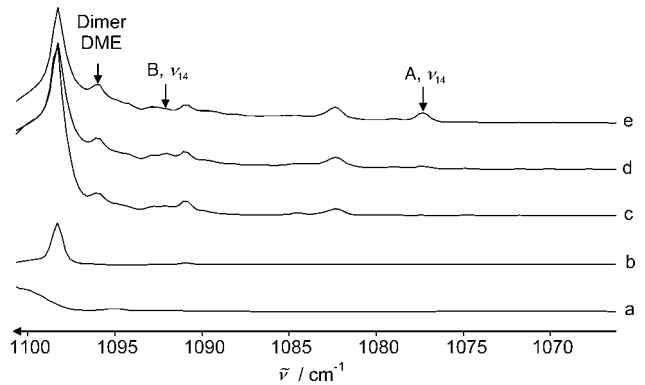

*Figure 4. IR spectra in the range 1065–1100 cm^{-1} of FA, DME, and FA/DME mixtures, matrix-isolated in argon. a) FA:Ar ratio 1:600, 13 K. b) DME:Ar ratio 1:600, 13 K. c) FA:DME:Ar ratio 1:1:600, 13 K. d) FA:DME:Ar ratio 1:1:600 after annealing at 25 K. e) FA:DME:Ar ratio 1:2:600 after annealing at 35 K. Vibrational modes assigned to FA/DME complexes are labeled **A** and **B**, respectively (see Tables 5 and 6).*

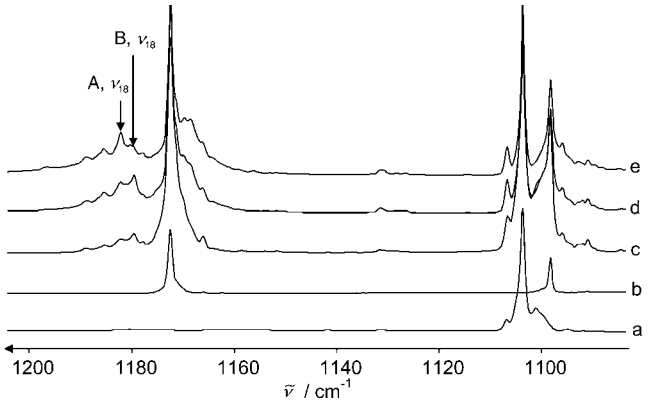

Figure 5. *IR spectra in the range 1080–1200 cm^{-1} of FA, DME, and FA/DME mixtures, matrix-isolated in argon. a) FA:Ar ratio 1:600, 13 K. b) DME:Ar ratio 1:600, 13 K. c) FA:DME:Ar ratio 1:1:600, 13 K. d) FA:DME:Ar ratio 1:1:600 after annealing at 25 K. e) FA:DME:Ar ratio 1:2:600 after annealing at 35 K. Vibrational modes assigned to FA/DME complexes are labeled **A** and **B**, respectively (see Tables 5 and 6).*

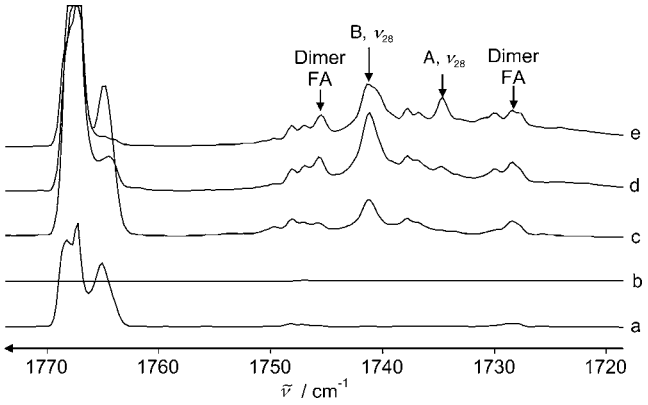

Figure 6. *IR spectra in the range 1720–1780 cm^{-1} of FA, DME, and FA/DME mixtures, matrix-isolated in argon. a) FA:Ar ratio 1:600, 13 K. b) DME:Ar ratio 1:600, 13 K. c) FA:DME:Ar ratio 1:1:600, 13 K. d) FA:DME:Ar ratio 1:1:600 after annealing at 25 K. e) FA:DME:Ar ratio 1:2:600 after annealing at 35 K. Vibrational modes assigned to FA/DME complexes are labeled A and B, respectively (see Tables 5 and 6).*

dimer **B** slightly decrease in intensity. Although it is tempting to assume that dimer **B** rearranges to **A** under these conditions the experiments do not unambiguously support this conclusion.

The IR spectra of complexes **A** and **B** were assigned by comparison with calculations at the MP2/cc-pVTZ level of theory (Tables 5 and 6). Characteristic for the formation of complexes of FA is the red shift of the C=O stretching vibration found at 1767.3 cm^{-1}. In the symmetrical doubly bridged dimer of FA the C=O stretching vibration is shifted by −38.6 cm^{-1}[36] and in the complex with water by −30.4 cm^{-1}.[38] In the complexes **A** and **B** these shifts are −32.3 and −26.1 cm^{-1}, respectively, and thus in the expected range (Figure 6). The experimental red-shifts are in excellent agreement with the MP2 calculations which predict shifts of −31.4 and −24.4 cm^{-1}, respectively, for the two complexes. The red-shifts in the C=O stretching vibration reflect the elongation of the C=O bond due to the formation of complexes. Obviously the interaction of the carbonyl oxygen atom in **A** with two DME hydrogen atoms is more efficient than the interaction with only one hydrogen atom as in complex **B**.

Due to a large number of absorptions in the region of the OH/CH stretching vibrations the assignment of bands to complexes **A** and **B** is very difficult and only tentative. For complex **A** the experimental O–H stretching frequency shift of −550 cm^{-1} is in excellent agreement with the calculated shift (−538 cm^{-1}) using MP2/cc-pVTZ (Table 5). For dimer **B** the calculated frequency shift (−449 cm^{-1}) also agrees very well with the experimental one (−473 cm^{-1}; Table 6) The large shifts of the O–H stretching vibrations allows to discard the FA–DME dimers **C**–**F** where the O–H···O interaction is lacking and thus the O–H stretching vibration of the FA molecule is much less perturbed (Figure 1).

The formation of hydrogen-bonded complexes of FA results in a contraction of the C–O bond and a blue-shift of the C–O stretching vibration found at 1104 cm^{-1} in the unperturbed molecule. For complex **A** a blue-shift of 89 cm^{-1} is predicted at the MP2/cc-pVTZ level of theory which matches the experimental value of 78 cm^{-1}. For complex **B** a shift of 91 cm^{-1} is predicted and 76 cm^{-1} are observed.

The DME molecule shows less pronounced shifts of IR absorptions due to the complex formation. The strong absorptions of monomeric DME and other constitutes in the matrix did not allow to identify C–H stretching vibrations of the DME molecule in the complexes. The asymmetric and symmetric C–O–C stretching vibration of both complexes **A** and **B** could be identified. In complex **A** the symmetrical C–O–C stretching vibration exhibits a red-shift of 25 cm^{-1} while the asymmetrical vibration is shifted by 15 cm^{-1}. This might be rationalized by the smaller distortion of the weak HOC(H)=O···HCH_2OCH_3 hydrogen bonds during the asymmetrical vibration as compared to the symmetrical vibration. In complex **B** the corresponding shifts are with 15 and 6 cm^{-1} smaller. The experimental red-shifts are in good agreement with the MP2 calculated values (Tables 5 and 6).

Conclusions

By using ab initio calculations six different bimolecular 1:1 complexes **A**–**F** of FA and DME could be identified. Two groups of complexes can be classified. One group consists of the complexes **A** and **B**, where the hydroxyl hydrogen atom of FA forms a strong hydrogen bond with the ether oxygen atom of DME. These two complexes are predicted to be the most stable ones and with 7.8–8 kcal mol^{-1} binding energy (MP2/cc-pVTZ + ZPE + BSSE, Table 1) to be almost isoenergetic. Comparison of the experimental data from matrix isolation experiments with calculated spectra indicated the formation of these two complexes. Although the OH···O interaction [type (1)] is dominating in complexes **A** and **B**, the secondary interaction between a methyl group hydrogen atom of DME and the carbonyl oxygen atom of FA [type (2)] leads to an additional significant stabilization of these complexes.

The second group of complexes **C**–**F** is defined by the absence of the strong hydrogen bond. With 2.3–2.9 kcal mol^{-1} (MP2/cc-pVTZ + ZPE + BSSE, Table 1) the binding energy is considerably smaller and consequently these complexes could not be identified experimentally. The dominant interaction in these complexes is the interaction between the formyl hydrogen atom of FA and the DME oxygen atom. Again, interactions between the methyl groups of DME and oxygen atoms of FA form secondary, weak interactions which, however, determine the geometry of the complexes.

Acknowledgments

This work was financially supported by the Deutsche Forschungsgemeinschaft (Sonderforschungsbereich 452) and the Fonds der Chemischen Industrie. We thank Dr. Holger Bettinger for helpful discussions.

Keywords: ab initio calculations · hydrogen bonds · IR spectroscopy · matrix isolation

[1] I. Agranat, N. V. Riggs, L. Radom, *J. Chem. Soc. Chem. Commun.* **1991**, 80 – 81.
[2] N. R. Brinkmann, G. S. Tschumper, G. Yan, H. F. Schaefer, *J. Phys. Chem. A* **2003**, *107*, 10 208 – 10 216.
[3] J. Chocholousova, J. Vacek, P. Hobza, *Phys. Chem. Chem. Phys.* **2002**, *4*, 2119 – 2122.
[4] H. Chojnacki, *Mol. Engineering* **1997**, *7*, 161 – 167.
[5] H. Ushiyama, K. Takatsuka, *J. Chem. Phys.* **2001**, *115*, 5903 – 5912.
[6] F. Madeja, M. Havenith, *J. Chem. Phys.* **2002**, *117*, 7162 – 7168.
[7] E. Sanchez-Garcia, L. George, L. A. Montero, W. Sander, *J. Phys. Chem. A* **2004**, *108,* 11 846 – 11 854.
[8] L. George, E. Sanchez-Garcia, W. Sander, *J. Phys. Chem. A* **2003**, *107*, 6850 – 6858.
[9] C. Zhu, Y. Ling, W. Y. Feng, C. Lifshitz, *Int. J. Mass Spectrom.* **2000**, *194*, 93 – 101.
[10] G. P. Ayers, A. D. E. Pullin, *Spectrochim. Acta, Part A* **1976**, *32A*, 1641 – 1650.
[11] M. L. H. Jeng, B. S. Ault, *J. Mol. Struct.* **1991**, *246*, 33 – 44.
[12] B. S. Ault, *J. Mol. Struct.* **2000**, *526*, 227 – 233.
[13] B. S. Ault, *Spectrochim. Acta A* **2003**, *59A*, 1989 – 1994.
[14] A. Engdahl, B. Nelander, *J. Chem. Soc. Faraday Trans.* **1992**, *88*, 177 – 182.
[15] B. C. Bricknell, T. M. Letcher, T. A. Ford, *South African J. Chem.* **1995**, *48*, 142 – 153.
[16] S. W. Han, K. Kim, *J. Mol. Struct.* **1999**, *475*, 43 – 53.
[17] J. Goebel, B. S. Ault, J. E. D. Bene, *J. Phys. Chem. A* **2000**, *104*, 2033 – 2037.
[18] A. Loutellier, L. Schriver, A. Burneau, J. P. Perchard, *J. Mol. Struct.* **1982**, *82*, 165 – 176.
[19] Gaussian 98 (Revision A.7), M. J. Frisch, G. W. Trucks, H. B. Schlegel, G. E. Scuseria, M. A. Robb, J. R. Cheeseman, V. G. Zakrzewski, J. A. Montgomery, R. E. Stratmann, J. C. Burant, S. Dapprich, J. M. Millam, A. D. Daniels, K. N. Kudin, M. C. Strain, O. Farkas, J. Tomasi, V. Barone, M. Cossi, R. Cammi, B. Mennucci, C. Pomelli, C. Adamo, S. Clifford, J. Ochterski, G. A. Petersson, P. Y. Ayala, Q. Cui, K. Morokuma, D. K. Malick, A. D. Rabuck, K. Raghavachari, J. B. Foresman, J. Cioslowski, J. V. Ortiz, B. B. Stefanov, G. Liu, A. Liashenko, P. Piskorz, I. Komaromi, R. Gomperts, R. L. Martin, D. J. Fox, T. Keith, M. A. Al-Laham, C. Y. Peng, A. Nanayakkara, C. Gonzalez, M. Challacombe, P. M. W. Gill, B. G. Johnson, W. Chen, M. W. Wong, J. L. Andres, M. Head-Gordon, E. S. Replogle, J. A. Pople, Gaussian, Inc., Pittsburgh, PA, **1998**.
[20] Gaussian 03 (Revision B.03),G. W. T. M. J. Frisch, H. B. Schlegel, G. E. Scuseria, J. R. C. M. A. Robb, J. A. Montgomery, Jr., T. Vreven, J. C. B. K. N. Kudin, J. M. Millam, S. S. Iyengar, J. Tomasi, B. M. V. Barone, M. Cossi, G. Scalmani, N. Rega, H. N. G. A. Petersson, M. Hada, M. Ehara, K. Toyota, J. H. R. Fukuda, M. Ishida, T. Nakajima, Y. Honda, O. Kitao, M. K. H. Nakai, X. Li, J. E. Knox, H. P. Hratchian, J. B. Cross, J. J. C. Adamo, R. Gomperts, R. E. Stratmann, O. Yazyev, R. C. A. J. Austin, C. Pomelli, J. W. Ochterski, P. Y. Ayala, G. A. V. K. Morokuma, P. Salvador, J. J. Dannenberg, S. D. V. G. Zakrzewski, A. D. Daniels, M. C. Strain, D. K. M. O. Farkas, A. D. Rabuck, K. Raghavachari, J. V. O. J. B. Foresman, Q. Cui, A. G. Baboul, S. Clifford, B. B. S. J. Cioslowski, G. Liu, A. Liashenko, P. Piskorz, R. L. M. I. Komaromi, D. J. Fox, T. Keith, M. A. Al-Laham, A. N. C. Y. Peng, M. Challacombe, P. M. W. Gill, W. C. B. Johnson, M. W. Wong, C. Gonzalez, J. A. Pople., Gaussian, Inc., Pittsburgh, PA, **2003**.
[21] C. Møller, M. S. Plesset, *Phys. Rev.* **1934**, *46*, 618 – 622.
[22] M. J. Frisch, J. A. Pople, J. S. Binkley, *J. Chem. Phys.* **1984**, *80*, 3265 – 3269.
[23] R. Krishnan, J. S. Binkley, R. Seeger, J. A. Pople, *J. Chem. Phys.* **1980**, *72*, 650 – 654.
[24] T. H. Dunning, Jr., *J. Chem. Phys.* **1989**, *90*, 1007 – 1023.
[25] S. F. Boys, F. Bernardi, *Mol Phys* **1970**, *19*, 553.
[26] L. A. Montero, A. M. Esteva, J. Molina, A. Zapardiel, L. Hernandez, H. Marquez, A. Acosta, *J. Am. Chem. Soc.* **1998**, *120*, 12 023 – 12 033.
[27] L. A. Montero, J. Molina, J. Fabian, *Int. J. Quantum Chem.* **2000**, *79*, 8 – 16.
[28] L. A. Montero, *GRANADA and Q programs for PC computers*, Laboratorio de Química Computacional y Teórica, Facultad de Química, Universidad de La Habana, Havana, Cuba, **1996** (available on request).
[29] J. J. P. Stewart, *J. Comput. Chem.* **1989**, *10*, 209 – 264.
[30] *MOPAC v 6.0 for PC Compute.*
[31] M. J. S. Dewar, E. G. Zoebisch, E. F. Healy, J. J. P. Stewart, *J. Am. Chem. Soc.* **1985**, *107*, 3902 – 3909.
[32] P. O. Astrand, G. Karlstrom, A. Engdahl, B. Nelander, *J. Chem. Phys.* **1995**, *102*, 3534 – 3554.
[33] D. Priem, T.-K. Ha, A. Bauder, *J. Chem. Phys.* **2000**, *113*, 169 – 175.
[34] Z. Zhou, Y. Shi, X. Zhou, *J. Phys. Chem. A* **2004**, *108*, 813 – 822.
[35] M. Halupka, W. Sander, *Spectrochim. Acta, Part A* **1998**, *54A*, 495 – 500.
[36] M. Gantenberg, M. Halupka, W. Sander, *Chem. Eur. J.* **2000**, *6*, 1865 – 1869.
[37] I. D. Reva, A. M. Plokhotnichenko, E. D. Radchenko, G. G. Sheina, Y. P. Blagoi, *Spectrochim. Acta A* **1994**, *50A*, 1107 – 1111.
[38] L. George, W. Sander, *Spectrochimica Acta A* **2004**, 3225 – 3232.
[39] M. D. Harmony, V. W. Laurie, R. L. Kuczkowski, R. H. Schwendeman, D. A. Ramsay, F. J. Lovas, W. J. Lafferty, A. G. Maki, *J. Phys. Chem. Ref. Data* **1979**, *8*, 619 – 721.

Received: September 9, 2004

